Journal of Colloid and Interface Science 458 (2015) 310–314

Contents lists available at ScienceDirect

Journal of Colloid and Interface Science

journal homepage: www.elsevier.com/locate/jcis

Short Communication

A methacrylate-based polymeric imidazole ligand yields quantum dots with low cytotoxicity and low nonspecific binding

Colin M. Johnson [a], Kayla M. Pate [b], Yi Shen [a], Anand Viswanath [a], Rui Tan [a], Brian C. Benicewicz [a,c], Melissa A. Moss [b,d], Andrew B. Greytak [a,c,*]

[a] Department of Chemistry and Biochemistry, University of South Carolina, Columbia, SC 29208, United States
[b] Department of Chemical Engineering, University of South Carolina, Columbia, SC 29208, United States
[c] USC Nanocenter, University of South Carolina, Columbia, SC 29208, United States
[d] Biomedical Engineering Program, University of South Carolina, Columbia, SC 29208, United States

GRAPHICAL ABSTRACT

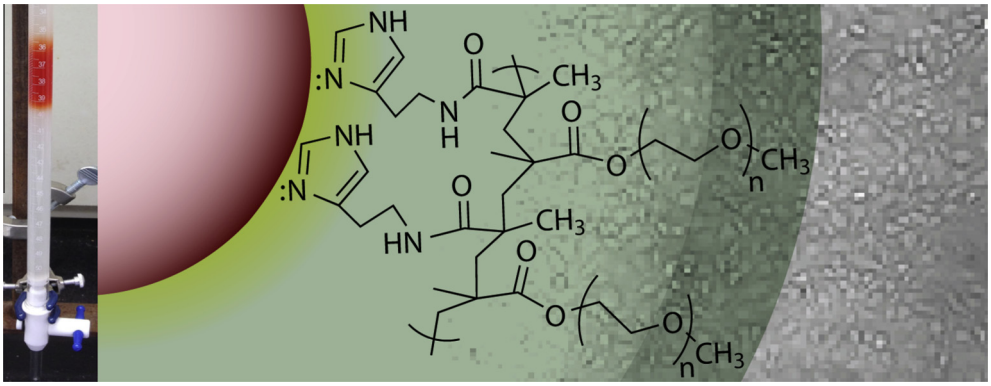

ARTICLE INFO

Article history:
Received 28 June 2015
Revised 28 July 2015
Accepted 30 July 2015
Available online 30 July 2015

Keywords:
CdSe
Core/shell quantum dots
Bio-imaging
Toxicity
Nonspecific binding
Fluorescence microscopy
Live cells
Ligand exchange
Polymer
Gel permeation chromatography

ABSTRACT

This paper assesses the biocompatibility for fluorescence imaging of colloidal nanocrystal quantum dots (QDs) coated with a recently-developed multiply-binding methacrylate-based polymeric imidazole ligand. The QD samples were purified prior to ligand exchange via a highly repeatable gel permeation chromatography (GPC) method. A multi-well plate based protocol was used to characterize nonspecific binding and toxicity of the QDs toward human endothelial cells. Nonspecific binding in 1% fetal bovine serum was negligible compared to anionically-stabilized QD controls, and no significant toxicity was detected on 24 h exposure. The nonspecific binding results were confirmed by fluorescence microscopy. This study is the first evaluation of biocompatibility in QDs initially purified by GPC and represents a scalable approach to comparison among nanocrystal-based bioimaging scaffolds.

Abbreviations: QD, quantum dot; GPC, gel permeation chromatography; FBS, fetal bovine serum; HUVEC, human umbilical vein endothelial cell; MA-PIL, methacrylate-based polymeric imidazole ligand; PEG, poly(ethylene glycol); DHLA, dihydrolipoic acid.

* Corresponding author at: Department of Chemistry and Biochemistry, University of South Carolina, Columbia, SC 29208, United States.
E-mail address: greytak@sc.edu (A.B. Greytak).

http://dx.doi.org/10.1016/j.jcis.2015.07.069
0021-9797/

1. Introduction

Colloidal nanocrystal quantum dots (QDs) offer size-tunable absorption and emission spectra [1], large molar extinction coefficients [2,3] and 2-photon excitation cross-sections [4,5], and high photostability [6,7] compared to most molecular fluorophores. These properties have led to intense interest in QDs as light emitters in bioimaging [5,7–10]. Requirements for biocompatible nanocrystals include high colloidal stability, minimized nonspecific binding to cell surfaces and other biological substrates, and low toxicity on relevant timescales. Hydrophilic organic ligand coatings have been demonstrated as a route to biocompatible QDs with smaller hydrodynamic radii than are achieved by encapsulation strategies [11–14]. A key challenge for ligand exchange strategies is to install strongly-binding ligands in a highly repeatable and modular manner. Recently, several groups have developed co-polymer ligands in which multiple functional groups providing QD chelation, water solubility, and/or handles for derivatization are pendant on a polymer backbone [15–19]. Multiply-binding polymeric ligands are designed to provide biocompatible QDs with increased stability compared to those terminated with small molecules bearing the same chelating groups, as well as a high degree of tunability on the basis of polymer composition and length. We recently described the synthesis of a series of polymeric imidazole ligands with a methacrylate backbone (MA-PILs) and their use in preparing water-soluble QDs [20]. The methacrylate monomers exhibit increased stability compared to acrylate monomers, facilitating the control of polymer ligand properties through RAFT polymerization kinetics.

Here, we evaluated the biocompatibility of a series of representative MA-PIL multiply-binding ligand formulations through scalable nonspecific binding and cell viability assays. To ensure a consistent QD starting material, we employed gel permeation chromatography (GPC) purification of the QDs [21] to remove impurities and weakly bound species prior to ligand exchange to install the MA-PIL ligand. The result illustrates the potential of methacrylate-based polymeric ligands to form biocompatible nanocrystals for targeting and sensing applications. Furthermore, these techniques and the results can serve as the basis for fundamental study and practical optimization of multiply-binding polymeric ligands for biomedical applications of inorganic nanoparticles.

2. Materials and methods

2.1. Materials

Wurtzite CdSe/CdZnS core/shell quantum dots and MA-PIL ligands were synthesized as described previously [20], PEG side-chains were incorporated using poly(ethylene glycol) methyl ether methacrylate 500 from Sigma–Aldrich. Bio-Beads S-X1 GPC medium was obtained from Bio-Rad Laboratories. Toluene-d_8 (D, 99.5%) was obtained from Cambridge Isotope Laboratories. Decylamine (95%) was purchased from Sigma Aldrich. Oleylamine (80–90%) and Bis(trimethylsilyl) sulfide ($(TMS)_2S$; 95%) were purchased from Acros Organics. Rhodamine 590 chloride (R590, MW 464.98) was obtained from Exciton. Toluene (99.5%) and Tetrahydrofuran (THF, 99%) were purchased from Mallinckrodt Chemicals. Ethanol (200 proof) was obtained from Decon Laboratories. Acetone (99.9%) was purchased from VWR. Methanol (99.9%) was purchased from Fisher Scientific. Toluene was dried with activated 4A molecular sieves. THF was dried using the Puresolv system from Innovative Technologies. Synthetic or analytical procedures under inert conditions were carried out using Schlenk line techniques or in a glovebox under N_2 atmosphere. All media components were from Sigma Aldrich. 96 well plates with clear plastic bottoms and black walls were obtained from VWR. Calcein AM was obtained from Invitrogen.

2.2. Preparation of MA-PIL coated quantum dots

Prior to ligand exchange, QDs (5 nmol) were purified by one cycle of precipitation and redissolution followed by GPC in toluene solvent. Toluene was then removed under vacuum, and chloroform added (0.3 mL) to form a clear solution. This QD solution was mixed with a solution of the MA-PIL ligand (175:1 mol ratio, for example ~30 mg for 34K MA-PIL), also in chloroform. After 30 min stirring at room temperature, a small amount of methanol was introduced followed by 30 min additional stirring. The QDs were then diluted with ethanol and hexane was introduced, causing precipitation of the ligand-exchanged QDs. The solution was decanted and QDs were redissolved in aqueous phosphate buffer solution (pH 7.4), and filtered (0.2 μm pore size). Finally, samples were dialyzed into deionized water via repeated centrifugal filtration with a 50,000 molecular weight cutoff membrane prior to biocompatibility experiments.

2.3. Cell culture and preparation

Human umbilical vein endothelial cells (HUVECs) (American Type Culture Collection) were maintained in Ham's F12K medium supplemented with 10% fetal bovine serum (FBS), 0.1 mg/mL heparin, 30 μg/mL endothelial cell growth supplement, 100 units/mL penicillin, and 100 μg/mL streptomycin. Prior to experimentation, HUVECs were seeded at a density of 5×10^4 cells/well onto black-sided 96-well tissue culture plates and maintained for 24 h in supplemented Ham's F12K medium with 1% FBS to allow formation of confluent monolayers. All cultures were maintained at 37 °C in a humid atmosphere of 5% CO_2 and 95% air.

2.4. Calcein AM cell viability assay

To characterize the potential toxicity of MA-PIL QDs, Calcein AM was used to assess cell viability following exposure to QDs. Confluent HUVEC monolayers were incubated (37 °C, 5% CO_2) with QDs coated with MA-PILs exhibiting effective molecular weights of 10K, 22K, or 34K. QD solutions were prepared by adding small aliquots of MA-PIL QD solutions in DI water to supplemented medium containing 1% FBS to achieve an ultimate concentration of 100 nM QDs. Monolayers incubated with equivalent dilution of DI water or with 25 μM cadmium acetate served as the vehicle and positive controls, respectively. Following 24 h incubation, treatments were decanted and replaced with 1 μM Calcein AM diluted in phenol red-free, serum-free media. When taken up by living cells, the non-fluorescent Calcein AM probe is hydrolyzed by endogenous esterases to yield fluorescent acetoxymethyl ester, thereby allowing for a quantifiable measurement of cell viability. After 1 h incubation (37 °C, 5% CO_2), fluorescence was measured using a BioTek Synergy 2 multi-mode microplate reader equipped with excitation and emission filters of 485 ± 20 nm and 530 ± 25 nm, respectively, and using baseline (media containing Calcein AM) subtraction. Cell viability is reported as Calcein AM fluorescence normalized to the fluorescence observed for the vehicle. Each treatment was performed in triplicate, and results shown are the mean ± SEM of three independent experiments.

2.5. Nonspecific binding assay

To evaluate nonspecific interactions between MA-PIL QDs and cells, a static adhesion assay was implemented. Confluent HUVEC monolayers were incubated for 5 min with MA-PIL QDs exhibiting molecular weights of 10K, 22K, or 34K. QD solutions were prepared

by adding small aliquots of MA-PIL QD solutions in DI water to supplemented medium containing 1% FBS to achieve an ultimate concentration of 200 nM. Incubations were performed at 4 °C to induce a state of cellular stasis, thereby preventing the endocytosis of MA-PIL QDs. Monolayers incubated with equivalent dilution of DI water or 200 nM of QDs coated with dihydrolipoic acid (DHLA) served as vehicle and positive control for nonspecific binding, respectively. Immediately following incubation, fluorescence was measured to serve as an internal positive control for each QD's self-fluorescence. Cells were then washed three times using PBS, pH 7.4, and fluorescence was measured again to evaluate nonspecific binding. Fluorescence was measured using a BioTek Synergy 2 multi-mode microplate reader equipped with excitation and emission filters of 530 ± 25 nm and 590 ± 35 nm, respectively. Fluorescence measurements were normalized to the fluorescence observed for the vehicle. Each experiment was performed with three replicates, and results are shown as the mean ± SEM of three to four independent experiments. To corroborate fluorescence results and assess sensitivity, monolayers were additionally imaged using a Nikon Eclipse Ti-E inverted microscope equipped with a 20× objective lens. Bright field and TRITC laser (excitation = 555 ± 10 nm; emission = 600 ± 20 nm) images were acquired for each sample. Images shown are representative of three to four independent experiments.

3. Results and discussion

The MA-PIL ligand includes multiple imidazole binding groups that could participate in a multidentate binding mode to the QD surface, poly(ethylene glycol) (PEG) chains to promote water solubility, and a methacrylate backbone [20]. Previous approaches to polymeric, multiply-binding ligands include modification of commercially available polyacrylic acid [18] and poly(maleic anhydrides) [17,19] with mixtures of thiols and/or imidazole binding groups, PEGs for water solubility, and/or functional handles; free-radical co-polymerization of thiol-functionalized methacrylates [16], and RAFT-mediated co-polymerization of functionalized acrylate monomers [15]. Controlled radical polymerization of functionalized monomers offers the ability to tune the polymer length and the distribution of functional sidechains within the polymers, which could be an advantage in producing optimized biocompatible QDs. The methacrylate backbone demonstrates advantages over previously used acrylate species [15], principally in the increased stability of methacrylate monomers against premature reactions. Free branched PEGs based on methacrylate backbones (PEG-MAs) have been shown to have low cytotoxicity [22], but the biocompatibility of QDs incorporating methacrylate backbones and imidazole binding groups has not been examined to our knowledge.

We applied three different formulations of the MA-PIL polymer to identical CdSe/CdZnS core/shell QD samples. The QD samples were purified by GPC using a toluene mobile phase and polystyrene size-exclusion medium. Importantly, this method has been shown to lead to QDs with low and consistent numbers of strongly-bound residual ligands [21], allowing the effects of subsequent ligand exchange procedures to be directly compared. The polymers tested had effective molecular weights, M_n, of 10,000, 22,000, and 34,000 as assigned from analytical GPC, with the difference in molecular weight reflecting the difference in the polymer chain length (average $N = 29$, 65, and 100 MA units). All polymers contained histamine and methoxy-terminated PEG-500 side chains at equal mole fractions; the ligand exchange with each of these ligand formulations resulted in clear solutions of QDs in water. Quantum yields measured in phosphate buffered saline at pH = 7.4 ranged from 22% to 32% with no clear dependence on M_n. Dynamic light scattering measurements of similarly-prepared MA-PIL QDs in water indicated hydrodynamic radii of ~8–9 nm [20].

We implemented two fluorescence-based assays to evaluate the biocompatibility of MA-PIL coated QDs under conditions that are typical of a cell-surface labeling experiment. The fluorescence-based assays were executed on a plate reader platform, permitting multiple replicates of each data point and potential scalability to a large number of polymer formulations to facilitate screening and optimization of putative biocompatible QDs. Since a common delivery method of QDs is via intravascular injection, in which the QDs come in contact with vascular endothelial cells, HUVEC cells have been utilized in a host of previous studies to assess QD toxicity [23–25]. In order to quantify the degree of cytotoxicity that the MA-PIL QDs elicited in HUVECs, a Calcein AM cell viability assay was utilized. The Calcein AM probe becomes fluorescent upon hydrolysis by esterases found in viable cells. Thus, cell viability can be assessed by the intensity of the fluorescence in the wells using a plate reader. Fig. 1 shows the fluorescence signal from wells containing monolayers treated with QDs coated with varying molecular weight MA-PILs (10K, 22K, 34K); fluorescence is normalized to the signal from wells with equivalent DI water (vehicle control). None of the cells treated with 100 nM QDs demonstrate a significant difference from vehicle after 24 h exposure. In addition, results were compared to a positive control in the form of a solution of 25 μM cadmium acetate. In soluble forms, cadmium is a highly cytotoxic and carcinogenic element; its presence in many varieties of nanocrystal QDs has been a source of concern in biological applications. Indeed, we observed significant toxicity for low micromolar concentrations of aqueous cadmium ion. In contrast, the total cadmium concentration in the QD samples is ~680 μM based on the number of Cd atoms per QD; the absence of toxicity by QDs suggests that Cd remains effectively sequestered in the QDs throughout the timescale of the experiment. We note that as free polymers, PEG-MA derivatives have been shown previously to exhibit very low cytotoxicity, comparable to or better than linear PEGs [26].

To assess the propensity of the MA-PIL QDs to bind nonspecifically, the samples were introduced at a relatively high

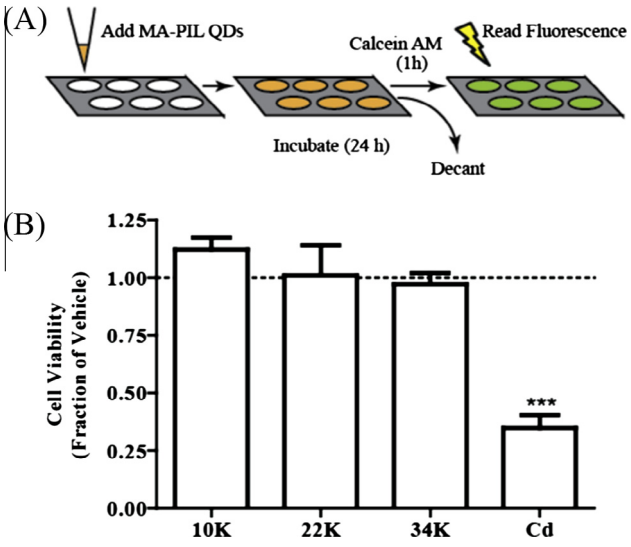

Fig. 1. Effect of MA-PIL QDs on cell viability. (A) HUVEC monolayers were incubated for 24 h (37 °C) with 100 nM QDs coated with MA-PIL ligands exhibiting molecular weights of 10K, 22K, or 34K or with 25 μM cadmium acetate (Cd, positive control). Cell viability was then assessed using Calcein AM. (B) Cell viability is reported as the experimental Calcein AM fluorescence normalized to the Calcein AM fluorescence observed for cells treated with vehicle only. Dashed line represents average cell viability of the vehicle. Error bars indicate SEM, $n = 3$. $^{***}p < 0.001$ *vs.* vehicle.

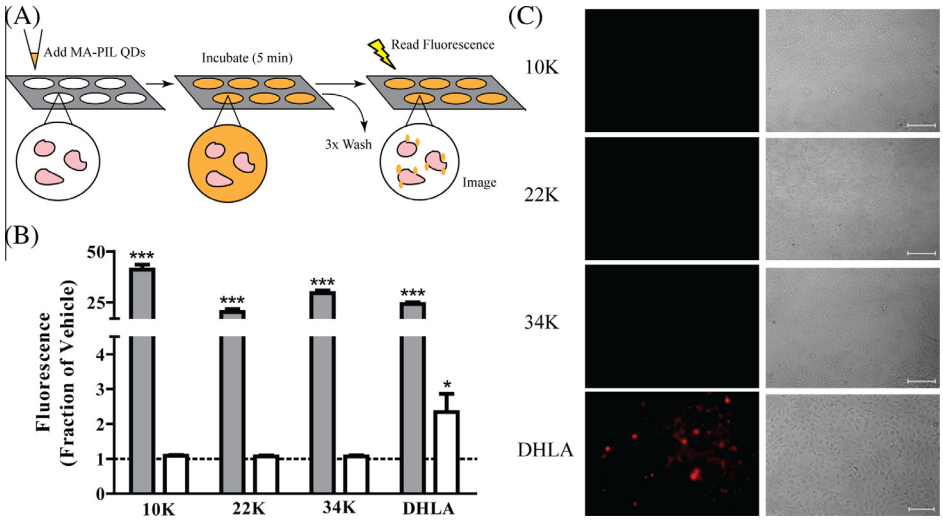

Fig. 2. Nonspecific binding of MA-PIL QDs to HUVEC monolayers. (A) HUVECs were incubated for 5 min at 4 °C with 200 nM QDs coated with MA-PIL ligands or with 200 nM QDs coated with DHLA ligands (positive control). The presence of MA-PIL QDs was quantified via self-fluorescence (panel B) and also visualized using fluorescence microscopy (panel C, left column). Fluorescence quantification was performed both before (grey bars) and following (white bars) three washes, with the latter representative of nonspecifically bound QDs. Phase contrast images (panel C, right column) were acquired to verify intact cell monolayers. Fluorescence was normalized to that observed for monolayers treated with a DI water equivalent (vehicle). Dashed line represents the normalized, average fluorescence observed for the vehicle. Error bars indicate SEM, $n = 3–4$. Some error bars lie within symbols. $^{*}p < 0.05$ and $^{***}p < 0.001$ *vs.* vehicle. Images are representative of 3–4 independent experiments; scale bars represent 200 μm.

concentration (200 nM) to HUVECs in medium containing 1% FBS and, following 5 min incubation, were decanted and rinsed so that any QDs that remained nonspecifically bound could be detected by virtue of their intrinsic fluorescence (Fig. 2A). In order to focus on nonspecific adsorption and avoid complications introduced by uptake via endocytosis, the incubation was conducted at low temperatures where endocytosis is less active. After three washes with PBS, the cells (treated with QDs with each coating, in triplicate) were analyzed via a plate reader to detect fluorescence at the QD emission channel. Any QDs remaining after the washes, for example as a result of nonspecific binding to cell surfaces or the culture substrate, will result in a contribution to the fluorescence that is absent in the wells exposed to vehicle only. Fig. 2B shows the plate reader results for each of the three MA-PIL QD samples. A fluorescence reading was also taken prior to washing, as an internal control for variation in the brightness of the QD samples. The results are expressed as a fraction of the vehicle. No significant increase in residual fluorescence was observed compared to vehicle (both sample and vehicle values include a similar small but non-zero contribution from autofluorescence and background).

The plate reader measurement provides a scalable, ensemble measurement of nonspecific binding that is immune to sampling bias that could be encountered in methods relying solely on fluorescence microscopy. As a positive control to confirm the ability of the method to detect nonspecific binding, we tested QDs coated with DHLA ligands. The carboxylate on DHLA is deprotonated at neutral pH, providing anionically stabilized QDs with a strongly negative zeta potential; DHLA-coated QDs have previously been observed to exhibit strong nonspecific binding to human cells [14]. Here, we confirm this observation with significant residual fluorescence detected at more than twice the vehicle.

In order to confirm that the ensemble measurement is sufficiently sensitive to detect nonspecific binding at a level that could interfere with the use of QDs for targeting cell imaging, the ensemble measurements were confirmed with live-cell fluorescence microscopy. In Fig. 2C, images are shown for each of the MA-PIL samples and the DHLA positive control. The left column shows the QD fluorescence channel images after washing away unbound QDs; the right column shows the bright field images after washing, which confirm intact endothelial monolayers. Under similar exposure conditions, the DHLA positive control showed localized QD fluorescence indicative of significant binding to cells, while no localized fluorescence contrast could be detected for any of the three MA-PIL QD samples.

4. Conclusions

Through assays designed to detect toxicity and nonspecific binding, we have demonstrated that polymeric imidazole ligands built on a polymethacrylate backbone are capable of producing water-soluble QDs with negligible short-term toxicity and negligible nonspecific adhesion to a human cells. The combination of GPC purification for the QD component [21] and RAFT-controlled polymerization of stable methacrylate monomers [20] represents a highly repeatable and potentially manufacturable route to biocompatible QDs with small hydrodynamic diameter, low nonspecific binding, and high fluorescence brightness. We showed that a well plate-based assay can detect nonspecific binding of QDs to a monolayer of cells. As such it can serve as a complement or alternative to microscopy-based assays.

The results shown here, for a binary copolymer with 50% PEGMA-500, demonstrate no significant difference in performance over the range of M_n studied. The scope of the MA-PIL ligand system is extensible to include ternary and end-functionalized copolymers that incorporate sites for derivatization under mild conditions, for example to form targeted QD probes. We believe this result will be a valuable point of reference for further optimization of biocompatible QDs, including those introducing specific targeting functions through introduction of bioaffinity groups or bio-orthogonal linking chemistries [27]. Additionally, the demonstration of biocompatibility in the PEG-MA motif of the polymer ligand could recommend a similar approach for surface treatment of other inorganic nanoparticles, including metals or oxides, for biological applications [28]. Non-specific binding is known to vary among cell lines [29] and to depend on buffer composition [30]. Future studies addressing specific bio-imaging objectives will motivate expansion of the scope of polymer compositions, cell lines, and buffer composition under which biocompatibility can be maintained with this system.

Acknowledgments

This research was supported by the University of South Carolina, including a SPARC Graduate Research Fellowship to YS, and a Magellan Scholarship and a SURF grant to CMJ. BCB acknowledges support from the SC SmartState program.

References

[1] A.M. Smith, S. Nie, Semiconductor nanocrystals: structure, properties, and band gap engineering, Acc. Chem. Res. 43 (2) (2010) 190–200.
[2] C.A. Leatherdale, W.-K. Woo, F.V. Mikulec, M.G. Bawendi, On the absorption cross section of CdSe nanocrystal quantum dots, J. Phys. Chem. B 106 (31) (2002) 7619–7622.
[3] J. Jasieniak, L. Smith, J. van Embden, P. Mulvaney, M. Califano, Re-examination of the size-dependent absorption properties of CdSe quantum dots, J. Phys. Chem. C 113 (45) (2009) 19468–19474.
[4] S.A. Blanton, M.A. Hines, M.E. Schmidt, P. Guyot-Sionnest, Two-photon spectroscopy and microscopy of II–VI semiconductor nanocrystals, J. Lumin. 70 (1–6) (1996) 253–268.
[5] D.R. Larson, W.R. Zipfel, R.M. Williams, S.W. Clark, M.P. Bruchez, F.W. Wise, W.W. Webb, Water-soluble quantum dots for multiphoton fluorescence imaging in vivo, Science 300 (5624) (2003) 1434–1436.
[6] X. Wu, H. Liu, J. Liu, K.N. Haley, J.A. Treadway, J.P. Larson, N. Ge, F. Peale, M.P. Bruchez, Immunofluorescent labeling of cancer marker Her2 and other cellular targets with semiconductor quantum dots, Nat. Biotechnol. 21 (1) (2003) 41–46.
[7] I.L. Medintz, H.T. Uyeda, E.R. Goldman, H. Mattoussi, Quantum dot bioconjugates for imaging. Labelling and sensing, Nat. Mater. 4 (6) (2005) 435–446.
[8] N. Erathodiyil, J.Y. Ying, Functionalization of inorganic nanoparticles for bioimaging applications, Acc. Chem. Res. 44 (10) (2011) 925–935.
[9] C.M. Lemon, P.N. Curtin, R.C. Somers, A.B. Greytak, R.M. Lanning, R.K. Jain, M.G. Bawendi, D.G. Nocera, Metabolic tumor profiling with pH, oxygen, and glucose chemosensors on a quantum dot scaffold, Inorg. Chem. 53 (4) (2014) 1900–1915.
[10] B. Zhang, R. Hu, Y. Wang, C. Yang, X. Liu, K.-T. Yong, Revisiting the principles of preparing aqueous quantum dots for biological applications: the effects of surface ligands on the physicochemical properties of quantum dots, RSC Adv. 4 (27) (2014) 13805–13816.
[11] H.T. Uyeda, I.L. Medintz, J.K. Jaiswal, S.M. Simon, H. Mattoussi, Synthesis of compact multidentate ligands to prepare stable hydrophilic quantum dot fluorophores, J. Am. Chem. Soc. 127 (11) (2005) 3870–3878.
[12] J.P. Zimmer, S.W. Kim, S. Ohnishi, E. Tanaka, J.V. Frangioni, M.G. Bawendi, Size series of small indium arsenide–zinc selenide core–shell nanocrystals and their application to in vivo imaging, J. Am. Chem. Soc. 128 (8) (2006) 2526–2527.
[13] W. Liu, H.S. Choi, J.P. Zimmer, E. Tanaka, J.V. Frangioni, M. Bawendi, Compact cysteine-coated CdSe(ZnCdS) quantum dots for in vivo applications, J. Am. Chem. Soc. 129 (47) (2007) 14530–14531.
[14] W. Liu, M. Howarth, A.B. Greytak, Y. Zheng, D.G. Nocera, A.Y. Ting, M.G. Bawendi, Compact biocompatible quantum dots functionalized for cellular imaging, J. Am. Chem. Soc. 130 (4) (2008) 1274–1284.
[15] W. Liu, A.B. Greytak, J. Lee, C.R. Wong, J. Park, L.F. Marshall, W. Jiang, P.N. Curtin, A.Y. Ting, D.G. Nocera, et al., Compact biocompatible quantum dots via RAFT-mediated synthesis of imidazole-based random copolymer ligand, J. Am. Chem. Soc. 132 (2) (2010) 472–483.
[16] I. Yildiz, E. Deniz, B. McCaughan, S.F. Cruickshank, J.F. Callan, F.M. Raymo, Hydrophilic CdSe–ZnS core–shell quantum dots with reactive functional groups on their surface, Langmuir 26 (13) (2010) 11503–11511.
[17] P. Zhang, S. Liu, D. Gao, D. Hu, P. Gong, Z. Sheng, J. Deng, Y. Ma, L. Cai, Click-functionalized compact quantum dots protected by multidentate-imidazole ligands: conjugation-ready nanotags for living-virus labeling and imaging, J. Am. Chem. Soc. 134 (20) (2012) 8388–8391.
[18] G. Palui, H.B. Na, H. Mattoussi, Poly(ethylene glycol)-based multidentate oligomers for biocompatible semiconductor and gold nanocrystals, Langmuir (2011).
[19] W. Wang, A. Kapur, X. Ji, M. Safi, G. Palui, V. Palomo, P.E. Dawson, H. Mattoussi, Photoligation of an amphiphilic polymer with mixed coordination provides compact and reactive quantum dots, J. Am. Chem. Soc. 137 (16) (2015) 5438–5451.
[20] A. Viswanath, Y. Shen, A.N. Green, R. Tan, A.B. Greytak, B.C. Benicewicz, Copolymerization and synthesis of multiply binding histamine ligands for the robust functionalization of quantum dots, Macromolecules 47 (23) (2014) 8137–8144.
[21] Y. Shen, M.Y. Gee, R. Tan, P.J. Pellechia, A.B. Greytak, Purification of quantum dots by gel permeation chromatography and the effect of excess ligands on shell growth and ligand exchange, Chem. Mater. 25 (14) (2013) 2838–2848.
[22] M. Chanana, S. Jahn, R. Georgieva, J.-F. Lutz, H. Baeumler, D. Wang, Fabrication of colloidal stable, thermosensitive, and biocompatible magnetite nanoparticles and study of their reversible agglomeration in aqueous milieu, Chem. Mater. 21 (9) (2009) 1906–1914.
[23] W.J.M. Mulder, R. Koole, R.J. Brandwijk, G. Storm, P.T.K. Chin, G.J. Strijkers, C. de Mello Donegá, K. Nicolay, A.W. Griffioen, Quantum dots with a paramagnetic coating as a bimodal molecular imaging probe, Nano Letters 6 (1) (2006) 1–6.
[24] M. Yan, Y. Zhang, K. Xu, T. Fu, H. Qin, X. Zheng, An in vitro study of vascular endothelial toxicity of CdTe quantum dots, Toxicology 282 (3) (2011) 94–103.
[25] S.J. Soenen, J. Demeester, S.C. De Smedt, K. Braeckmans, The cytotoxic effects of polymer-coated quantum dots and restrictions for live cell applications, Biomaterials 33 (19) (2012) 4882–4888.
[26] J.-F. Lutz, Polymerization of Oligo(ethylene Glycol) (meth)acrylates: toward new generations of smart biocompatible materials, J. Polym. Sci. Part Polym. Chem. 46 (11) (2008) 3459–3470.
[27] H.-S. Han, E. Niemeyer, Y. Huang, W.S. Kamoun, J.D. Martin, J. Bhaumik, Y. Chen, S. Roberge, J. Cui, M.R. Martin, et al., Quantum dot/antibody conjugates for in vivo cytometric imaging in mice, Proc. Natl. Acad. Sci. 112 (5) (2015) 1350–1355.
[28] N. Chan, M. Laprise-Pelletier, P. Chevallier, A. Bianchi, M.-A. Fortin, J.K. Oh, Multidentate block-copolymer-stabilized ultrasmall superparamagnetic iron oxide nanoparticles with enhanced colloidal stability for magnetic resonance imaging, Biomacromolecules 15 (6) (2014) 2146–2156.
[29] S. Laurent, C. Burtea, C. Thirifays, U.O. Häfeli, M. Mahmoudi, Crucial ignored parameters on nanotoxicology: the importance of toxicity assay modifications and "Cell Vision", PLoS ONE 7 (1) (2012) e29997.
[30] C.C. Fleischer, C.K. Payne, Nanoparticle-cell interactions: molecular structure of the protein corona and cellular outcomes, Acc. Chem. Res. 47 (8) (2014) 2651–2659.